Derivation of enhanced potentials for plutonium dioxide and the calculation of lattice and intrinsic defect properties

CrossMark

Mark S.D. Read [a,*], Scott R. Walker [b], Robert A. Jackson [b]

[a] School of Chemistry, University of Birmingham, Edgbaston, Birmingham B15 2TT, United Kingdom
[b] School of Physical and Geographical Sciences, Keele University, Keele, Staffs ST5 5BG, United Kingdom

ARTICLE INFO

ABSTRACT

A new potential has been derived for plutonium dioxide and used to calculate its lattice and defect properties. The $Pu^{4+} \cdots O^{2-}$ potential is obtained *via* a combination of empirical fitting to crystal structural data and parametric fitting to additional physical properties, while the $O^{2-} \cdots O^{2-}$ potential is transferred from an earlier publication on UO_2. The overall potential is subsequently verified and validated by calculation of elastic and dielectric constants, whose values agree favourably with those measured experimentally. Calculations are then presented of the intrinsic defect formation energies and predictions of the expected type of intrinsic disorder made.

© 2014 Elsevier B.V. All rights reserved.

1. Introduction

Plutonium ceramics are becoming increasingly important in nuclear fuel cycles with plutonium dioxide (PuO_2) receiving renewed attention recently following a nuclear renaissance driven by the United Kingdom (UK) Government's commitment to reduce CO_2 emissions from the combustion of carbon based fuels [1]. Indeed, new nuclear power is essential to meeting the Governments objective of delivering a secure, sustainable and low-carbon energy future [2].

Moreover, a large amount of PuO_2 is in storage around the world, including a significant stockpile at the Sellafield site (UK). "The vast majority of UK PuO_2 derives from reprocessing of spent uranium metal fuels from UK Magnox reactors ("Magnox" PuO_2) or reprocessing of spent oxide fuels from UK Advanced Gas Cooled reactors or foreign light water reactors in the Thorp reprocessing plant ("Thorp" PuO_2)" [3]. The UK stockpile has accumulated over the last ≈ 50 years and the UK Government is now considering eventual re-use of this Pu as Mixed Oxide (MOX) fuel for thermal reactors [4–6].

PuO_2 mixed with UO_2 has already endured service in thermal reactors with the mixtures performing well. Because of the interest in fast reactors and space systems, fuels containing higher concentrations of plutonium oxides will require development. Indeed, interest in the use of Mixed Oxide (MOX) fuels comprising $(U, Pu, MA)O_2$ (where MA = Np, Am and Cm) in fast breeder and transmutation reactors is ever increasing.

Atomistic computer simulation techniques remain complementary to experimental methods and are ideally suited to provide fundamental insight into the defect chemistry. In view of the importance of PuO_2, there remains a strong incentive for reliable theoretical studies.

In this paper similar methods to those adopted in a previous paper on UO_2 [7] are applied to PuO_2 in order to obtain information about its lattice properties and defect behaviour. This is an important preliminary step in modelling MOX fuel which is the subject of ongoing work and a later publication.

2. Computational techniques

2.1. Introduction

The computer modelling techniques employed in this paper have been used in studying a wide range of materials, from actinide oxides [8] to mixed metal fluorides [9]. The basic idea is the use of interatomic potentials to define interactions in the material, with the potential parameters being obtained by empirical fitting. The analytical form of potential that has been used is the Buckingham potential, supplemented by an electrostatic interaction term:

$$V_{ij} = \underbrace{A_{ij} \exp\left(-\frac{r_{ij}}{\rho_{ij}}\right) - \frac{C_{ij}}{r_{ij}^6}}_{\text{Buckingham}} + \underbrace{\frac{q_i q_j}{r_{ij}}}_{\text{Electrostatic}} \qquad (1)$$

* Corresponding author. Tel.: +44 01214147813.
E-mail addresses: m.s.d.read@bham.ac.uk (M.S.D. Read), s.r.walker@keele.ac.uk (S.R. Walker), r.a.jackson@keele.ac.uk (R.A. Jackson).

Here, the parameters A, ρ and C are specified for each interaction type, and q_i and q_j are the charges of the interacting ions. The procedure for obtaining the potential parameters is described in the next section.

2.2. Fitting the potential

PuO$_2$ and UO$_2$ adopt the same cubic crystal structure and thus the anions are arranged with the same symmetry within unit cells of a similar size. Thus, the interactions between anions may be described in PuO$_2$ in the same manner as employed for UO$_2$, *i.e.* by a four-range Buckingham potential [10]. This is not an unreasonable assumption and indeed this approach has been used elsewhere for the derivation of empirical potential parameters for binary oxides by Lewis and Catlow [11].

Because of the hazardous nature of PuO$_2$, only a small number of experimental observations are accessible with which to perform empirical fitting. Crystallographic data are reported by Belin *et al.* [12]. The high frequency dielectric constant [13] and certain Raman data [14] are available. However, in the absence of experimental observation, previously published theoretical predictions for PuO$_2$ [10,15] act as a guide to the fitting of elastic matrix elements (C_{ij}) and the static dielectric constant.

The procedure used to obtain the potential parameters between the cation and anion requires no *a priori* assumption of starting values and is described in detail in the previous publication on UO$_2$ [7]. The main features of these calculations are recalled briefly as follows.

The procedure surveys the potential landscape with appropriate values for the A and ρ parameters being selected in a sequential manner. The initial stage of this process involves screening a range of A and ρ values and observing the difference between predicted and observed structural properties. Fig. 1 illustrates the potential surface by plotting the difference between predicted and observed PuO$_2$ lattice constant (a_0) for a range of A (750–2100 eV) and ρ (0.35–0.43 Å) values. The surface mesh is interpolated to obtain combinations which reproduce a_0 exactly (*i.e.* where $\delta = 0$) as indicated by red circular markers.

It is of interest to note that within this selected range a multitude of pairs of values reproduce the crystal structure. Zero contour points are interpolated to form the solution set shown in Fig. 2.

However, a pair which also describe the physical characteristics of the lattice are required for a reliable and robust model. Thus, elastic constants predicted from this solution set are subsequently investigated. Predicted elastic constants (C_{11}, C_{12} and C_{44}) are plot-
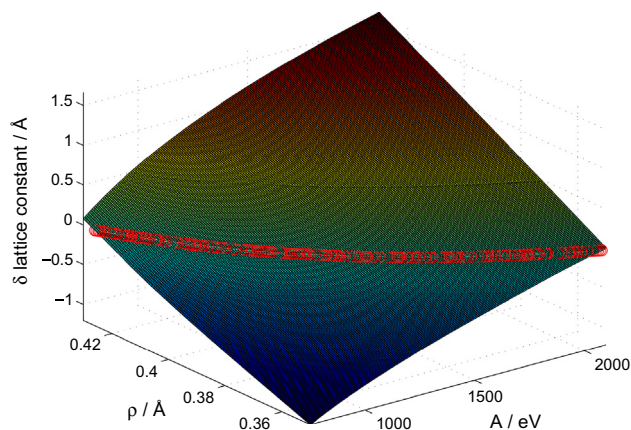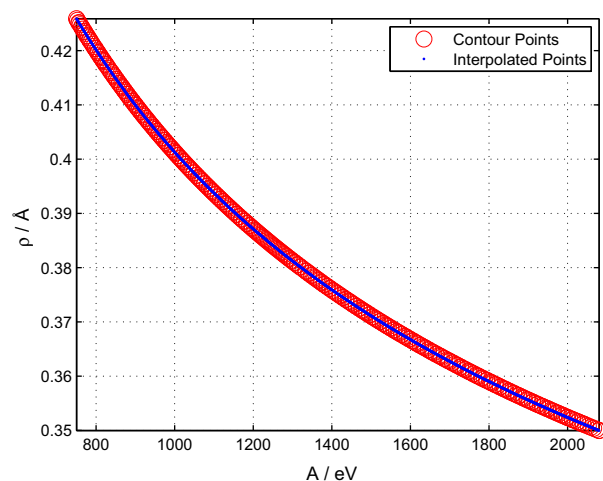

Fig. 2. Zero contour points and interpolated values of A and ρ comprising the solution set.
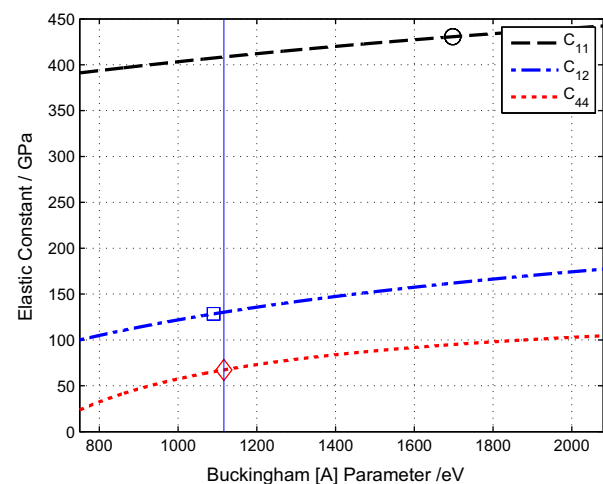

Fig. 3. Plot of predicted and observed elastic constants as a function of A.

ted as a function of the A parameter component of the solution set in conjunction with observed values, as shown in Fig. 3.

The second stage plots series of predicted elastic constants as a function of A terms from corresponding A/ρ pairs within the solution set. Fig. 4 plots the individual and mean percentage difference between predicted and observed values for the elastic constants and a value of A is selected where the mean square difference is a minimum, *i.e.* at 1116.3317 eV.

Having determined the value for A, the corresponding ρ value is interpolated from the solution set (Fig. 5) to provide the pair of variables for the desired potential.

Dielectric properties are of crucial importance in many contexts, including those beyond the strictly bulk properties. For example, the response of a solid to a charged defect depends on the inverse of the dielectric constant. The actual value of the dielectric constant varies according to the frequency of the electromagnetic field applied. Commonly, two extreme values are quoted, namely the static (ε_0) and high frequency (ε_∞) dielectric constants. In the static limit all degrees of freedom of the crystal, both nuclear and electronic, are able to respond to the electric field and therefore to provide screening. At the high frequency limit the oscillation is greater than the maximum vibrational frequency of the

Fig. 1. Plot of the difference between predicted and observed PuO$_2$ lattice constant for A and ρ values of the Pu$^{4+}\cdots$O^{2-} Born–Mayer potential.